

Electronic Supplementary Information (ESI) for

Reversible and irreversible reaction mechanisms of Li-CO₂ batteries

Xinxin Zhang, Yu Wang,* and Yafei Li*

Jiangsu Key Laboratory of New Power Batteries, Jiangsu Collaborative Innovation Centre of Biomedical Functional Materials, School of Chemistry and Materials Science, Nanjing Normal University, Nanjing 210023, P. R. China.

To whom correspondence should be addressed. E-mail: yu.wang@njnu.edu.cn;
liyafei@njnu.edu.cn(YL)

Table of the contents:

1. Supporting Figures S1–S14
2. Supporting Tables S1-S3

1. Supporting Figures S1–S14

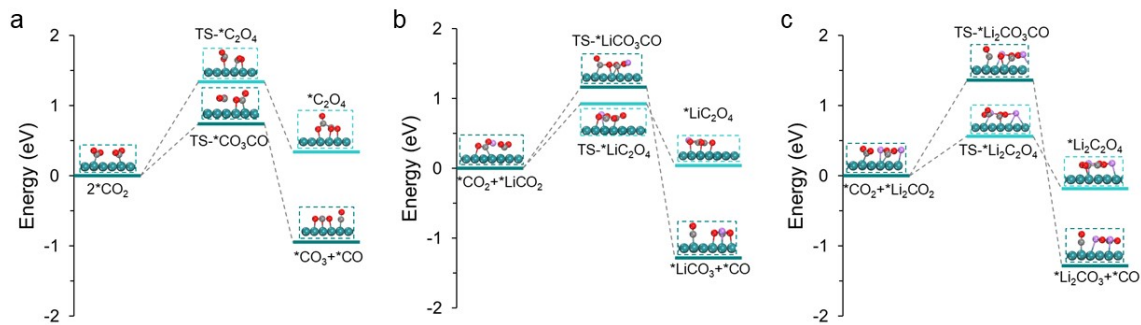


Fig. S1 Energy barriers and related geometric structures of the disproportionation of (a) $*\text{CO}_2$, (b) $*\text{LiCO}_2$, and (c) $*\text{Li}_2\text{CO}_2$ on Ru(0001).

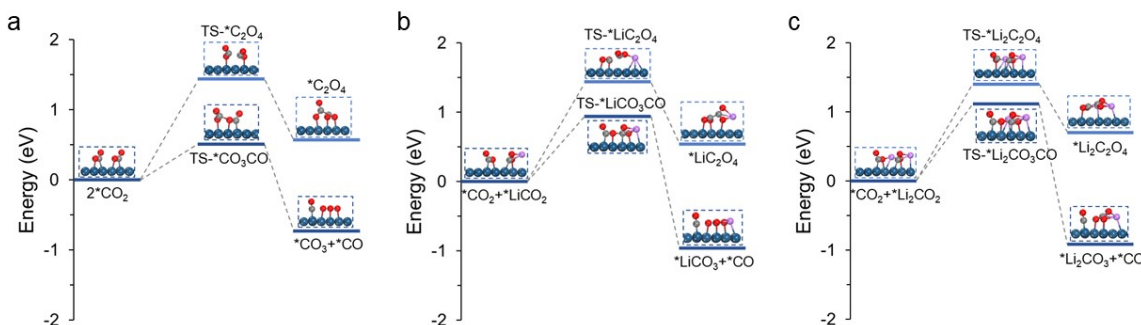


Fig. S2 Energy barriers and related geometric structures of the disproportionation of (a) $*\text{CO}_2$, (b) $*\text{LiCO}_2$, and (c) $*\text{Li}_2\text{CO}_2$ on Ir(111).

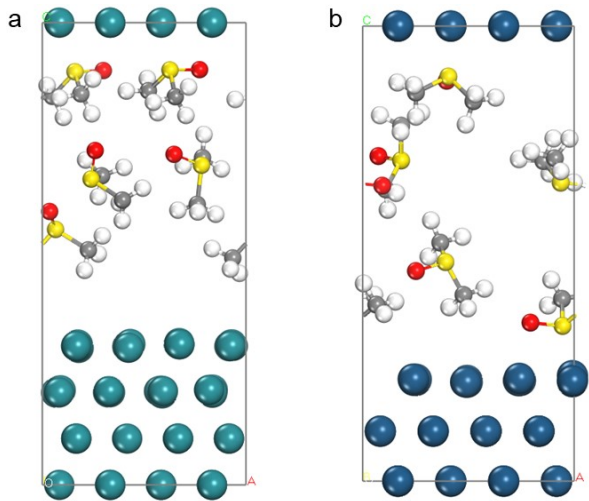


Fig. S3 (a,b) Simulation box of the (a) Ru(0001), and (b) Ir(111) systems with explicit DMSO molecules.

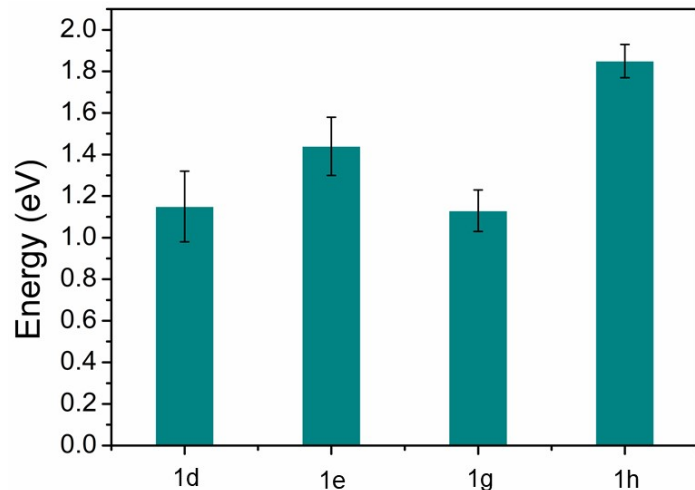


Fig. S4 The error bars of the CO_2 disproportionation and dimerization pathways on Ru(0001) and Ir(111).

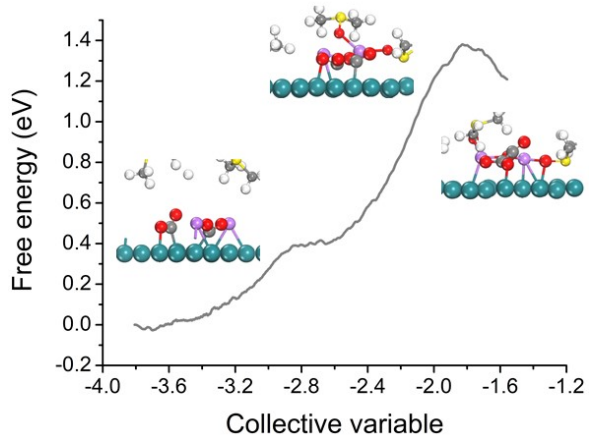


Fig. S5 Free energy profile for the reduction of $^{*}\text{CO}_2$ and $^{*}\text{Li}_2\text{CO}_2$ on the Ru(0001) surface.

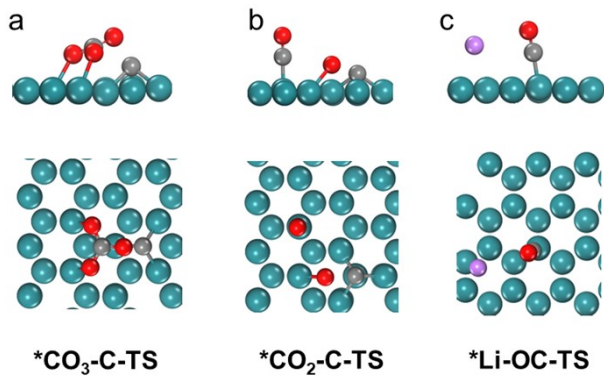


Fig. S6 The enlarged spots of the transition states of (a) $^{*}\text{CO} + ^{*}\text{CO}_2 \rightarrow ^{*}\text{CO}_3 + ^{*}\text{C}$, (b) $2^{*}\text{CO} \rightarrow ^{*}\text{CO}_2 + ^{*}\text{C}$, and (c) $^{*}\text{CO} + \text{Li}^+ + \text{e}^- \rightarrow ^{*}\text{LiOC}$ on Ru(0001).

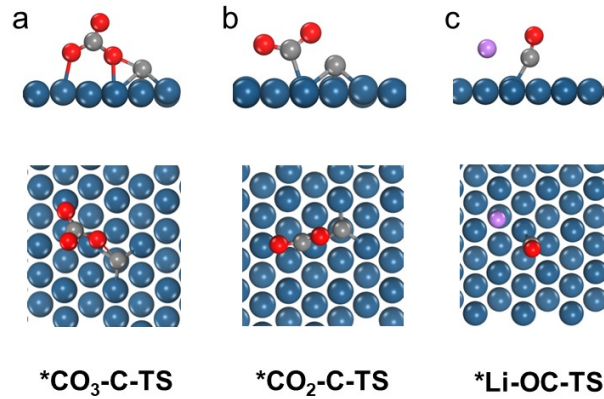


Fig. S7 The enlarged spots of the transition states of (a) $^*\text{CO} + ^*\text{CO}_2 \rightarrow ^*\text{CO}_3 + ^*\text{C}$, (b) $2^*\text{CO} \rightarrow ^*\text{CO}_2 + ^*\text{C}$, and (c) $^*\text{CO} + \text{Li}^+ + \text{e}^- \rightarrow ^*\text{LiOC}$ on Ir(111).

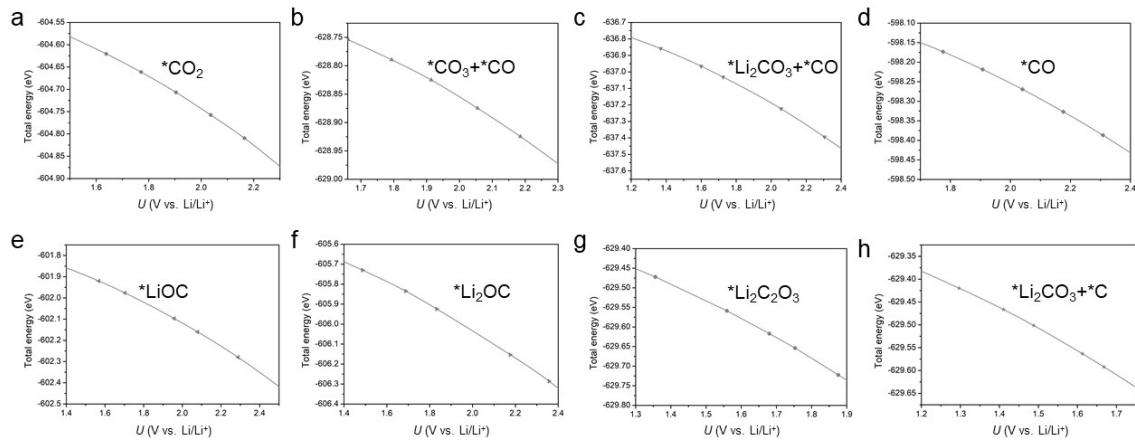


Fig. S8 (a-h) Total energy of absorbed intermediates of Ru(0001) as a function of potential.

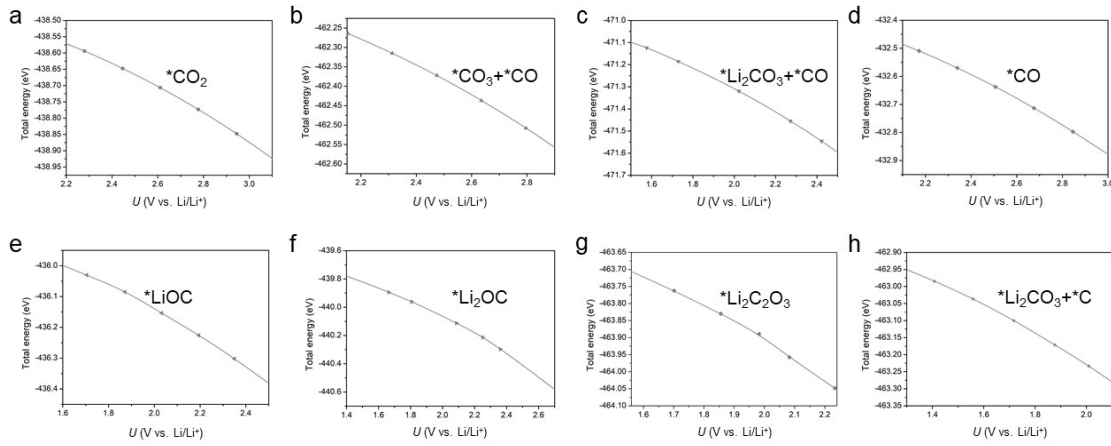


Fig. S9 (a-h) Total energy of absorbed intermediates of Ir(111) as a function of potential.

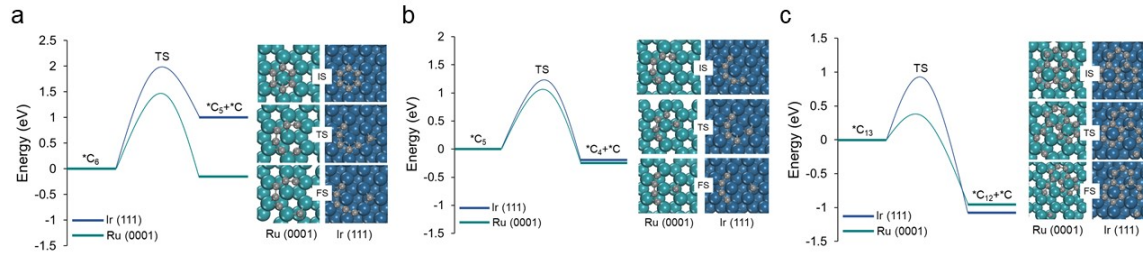


Fig. S10 Energy barriers of removing a C atom from (a) C₆ cluster, (b) C₅ cluster, and (c) C₁₃ cluster on Ru(0001) and Ir(111).

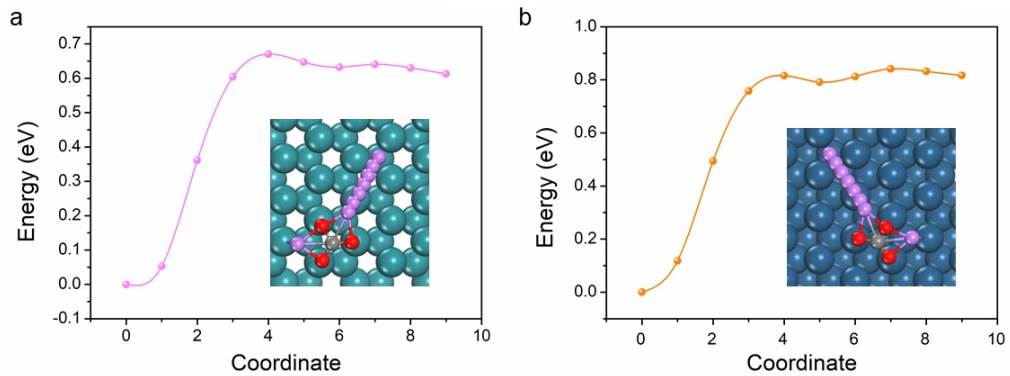


Fig. S11 Energy barrier diagrams for Li₂CO₃ delithiation on (a) Ru(0001) and (b) Ir(111).

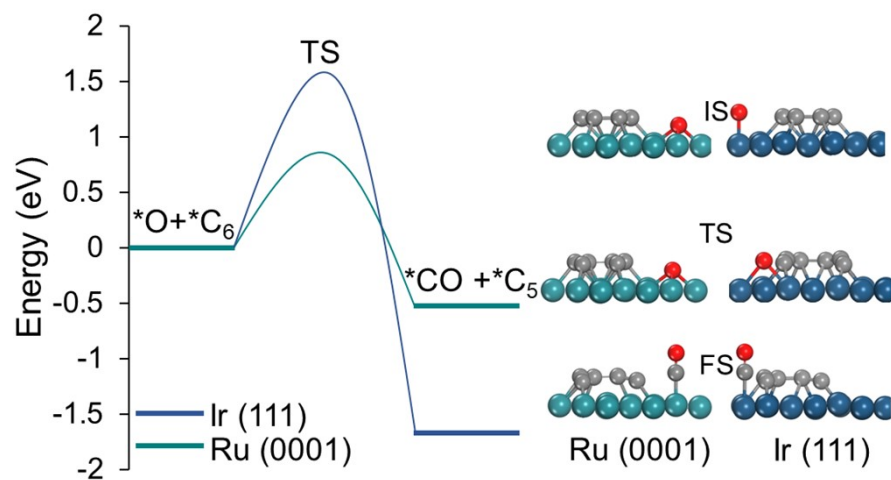


Fig. S12 Energy barriers for the oxidative decomposition of ^{*}C₆ to form ^{*}C₅ and ^{*}CO on Ru(0001) and Ir(111).

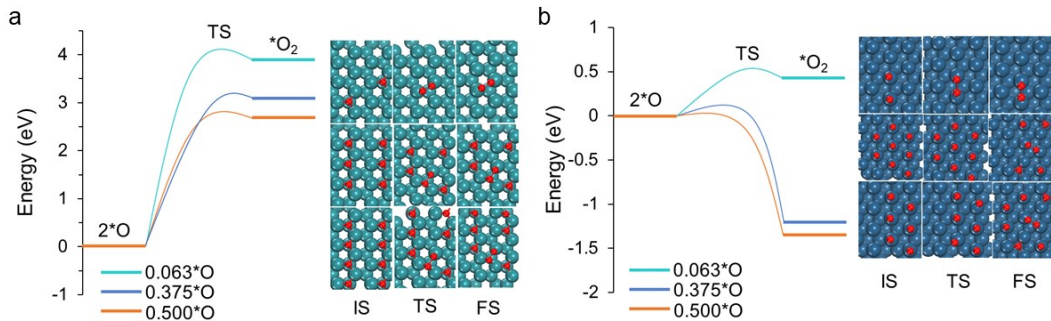


Fig. S13 Energy barriers for *O oxidation under different *O coverages on (a) Ru(0001) and (b) Ir(111).

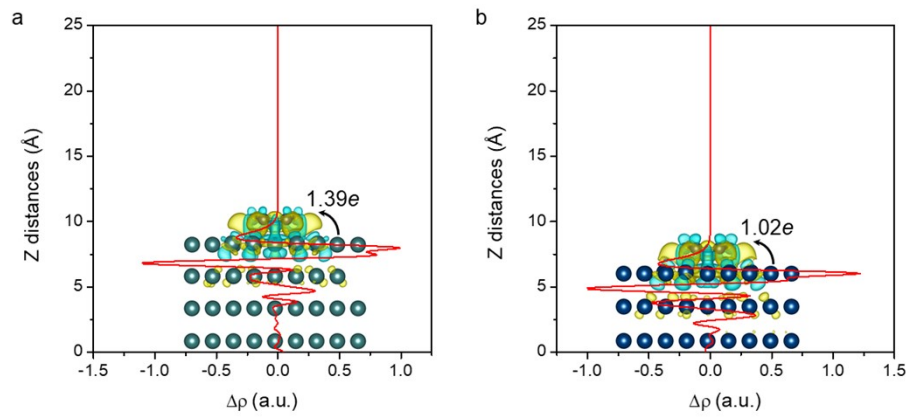


Fig. S14 The local integral curve of electron density difference along the Z direction. The difference in charge density of C adsorbed on (a) Ru(0001) and (b) Ir(111). The yellow and cyan represent the increase and decrease of electron density, respectively. The isosurface is 0.003 a.u.

2. Supporting Tables S1-S3

Table S1. Free energy changes (ΔG) of each reaction step on the Ru (0001) and Ir (111) surfaces (corresponding to Figure 2).

Reaction Step	ΔG for Ru (0001) (eV)	ΔG for Ir (111) (eV)
$* + \text{CO}_2 \rightarrow * + \text{CO}_2$	0.02	0.23
$* \text{CO}_2 + \text{CO}_2 \rightarrow * \text{CO}_3 + * \text{CO}$	-0.97	-0.34
$* \text{CO}_3 + * \text{CO} + \text{Li}^+ + e^- \rightarrow * \text{LiCO}_3 + * \text{CO}$	-2.06	-2.28
$* \text{LiCO}_3 + * \text{CO} + \text{Li}^+ + e^- \rightarrow * \text{Li}_2\text{CO}_3 + * \text{CO}$	-1.87	-2.51
$* \text{Li}_2\text{CO}_3 + * \text{CO} \rightarrow \text{Li}_2\text{CO}_3 + * \text{CO}$	-1.13	-1.13
$* \text{CO} + \text{Li}^+ + e^- \rightarrow * \text{LiOC}$	-1.43	-1.54
$* \text{LiOC} + \text{Li}^+ + e^- \rightarrow * \text{Li}_2\text{OC}$	-1.89	-1.69
$* \text{Li}_2\text{OC} + \text{CO}_2 \rightarrow * \text{Li}_2\text{C}_2\text{O}_3$	-0.64	-0.65
$* \text{Li}_2\text{C}_2\text{O}_3 \rightarrow * \text{Li}_2\text{CO}_3 + * \text{C}$	0.07	0.66
$* \text{CO} + \text{CO} \rightarrow * \text{CO}_2 + * \text{C}$	-0.41	0.37
$* \text{CO} + \text{CO}_2 \rightarrow * \text{CO}_3 + * \text{C}$	0.42	1.33

Table S2. Free energy changes (ΔG) of the reaction steps on the Ru (0001) surface (corresponding to Figure 4).

	Reaction step	ΔG for Ru (0001) (eV)
S2- I	$C + *Li_2CO_3 \rightarrow C + *CO_3 + 2Li^+ + 2e^-$	3.94
	$C + *CO_3 \rightarrow *CO_2 + *O + C$	-0.53
	$C + *CO_2 + *O \rightarrow CO_2 + *O + C$	-0.02
	$*O + C \rightarrow *CO$	-0.52
	$*CO + *O \rightarrow *CO_2$	1.49
S2- II	$*O + *O \rightarrow *O_2$	3.90

Table S3. Free energy changes (ΔG) of the reaction steps on the Ir (111) surface (corresponding to Figure 4).

	Reaction step	ΔG for Ir (111) (eV)
S2- I	$*Li_2CO_3 \rightarrow *CO_3 + 2Li^+ + 2e^-$	4.78
	$*CO_3 \rightarrow *CO_2 + *O$	0.32
	$*CO_2 + *O \rightarrow CO_2 + *O$	-0.23
	$*O + C \rightarrow *CO$	-1.60
	$*O + *O \rightarrow *O_2$	0.43

